IEEE Access
Multidisciplinary | Rapid Review | Open Access Journal

Received April 6, 2020, accepted May 11, 2020, date of publication May 19, 2020, date of current version June 3, 2020.

Digital Object Identifier 10.1109/ACCESS.2020.2995783

Wireless Power Transfer System for Battery-Less Sensor Nodes

BILAL TARIQ MALIK[1,2], (Graduate Student Member, IEEE),
VIKTOR DOYCHINOV[2], ALI MOHAMMAD HAYAJNEH[2,3], (Member, IEEE),
SYED ALI RAZA ZAIDI[2], (Member, IEEE),
IAN D. ROBERTSON[2], (Fellow, IEEE),
AND NUTAPONG SOMJIT[2], (Senior Member, IEEE)

[1]Department of Electrical and Computer Engineering, COMSATS University Islamabad, Islamabad 45550, Pakistan
[2]School of Electronics and Electrical Engineering, University of Leeds, Leeds LS2 9JT, U.K.
[3]Department of Electrical Engineering, The Hashemite University, Zarqa 13133, Jordan

Corresponding author: Viktor Doychinov (v.o.doychinov@leeds.ac.uk)

This work was supported in part by the Engineering and Physical Sciences Research Council, U.K., under Grant EP/N010523/1 and Grant EP/S016813/1.

ABSTRACT For the first time, the design and implementation of a fully-integrated wireless information and power transfer system, operating at 24 GHz and enabling battery-less sensor nodes, is presented in this paper. The system consists of an RF power source, a receiver antenna array, a rectifier, and a battery-less sensor node which communicates via backscatter modulation at 868 MHz. The rectifier circuits use commercially available Schottky diodes to convert the RF power to DC with a measured efficiency of up to 35%, an improvement of ten percentage points compared with previously reported results. The rectifiers and the receive antenna arrays were jointly designed and optimised, thereby reducing the overall circuit size. The battery-less sensor transmitted data to a base station realised as a GNU Radio flow running on a bladeRF Software Defined Radio module. The whole system was tested in free-space in laboratory conditions and was capable of providing sufficient energy to the sensor node in order to enable operation and wireless communication at a distance of 0.15 metres.

INDEX TERMS Millimeter-wave engineering, rectifiers, wireless power transfer, battery-less, sensors.

I. INTRODUCTION

The research field of wireless power transfer (WPT) has attracted considerable attention due to the novel battery-free solutions it could enable in many emerging applications across different domains such as infrastructure robotics, Internet of Things (IoT) devices, and sensor networks [1], [2]. A lot of results have already been reported for WPT circuits and systems operating in the sub-6 GHz frequency bands such as 433 MHz, 868 MHz, and 2.4 GHz. Research and development effort has now shifted towards higher frequencies partially due to improved directivity achievable through the use of antennas with electrically larger apertures [3]–[5].

The two major requirements of an efficient wireless power transfer system are a high-gain directional antenna and a rectifier circuit with high RF-DC conversion efficiency [2]. A rectenna is the combination of a receive antenna and a rectifier that together form a complete WPT receiver [1], [5]. The overall performance of a WPT system directly depends on the overall efficiency of the rectenna [6]. In addition to the RF-DC conversion efficiency, other relevant comparison metrics of rectifiers are DC output voltage and required input RF power level.

While traditionally rectifier and rectenna articles have focused on using sub-6 GHz frequencies, those above 6 GHz offer several advantages. One of the main benefits is the reduction in the physical space occupied by the rectennas, while retaining the high gain and narrow beamwidth [6]. The higher frequency WPT is suitable for applications where there are constraints on the size of the antennas, such as on board unmanned aerial vehicles (UAVs), infrastructure pipe inspection robots, and small battery-less sensor nodes. Higher frequency WPT may also be safer in terms of human exposure, up to a reasonable power level, because the energy

The associate editor coordinating the review of this manuscript and approving it for publication was Vittorio Camarchia.

This work is licensed under a Creative Commons Attribution 4.0 License. For more information, see https://creativecommons.org/licenses/by/4.0/

is primarily absorbed by the surface layers of the skin [7], [8]. WPT in the 24 GHz Industrial, Scientific, and Medical (ISM) band has the major advantage that it will not interfere with other frequency bands, which are widely used for communication purposes, such as millimetre-wave 5G frequencies. The drawbacks of using 24 GHz include increased propagation and atmospheric losses, as well as less efficient semiconductor components. These can however be outweighed by commensurate increase in directivity and gain of antennas, in addition to other system requirements such as reduced circuit footprint.

Various rectifier and rectenna designs have been proposed in the existing literature. Bito *et al.* [9] demonstrated a flexible, ink-jet printed millimetre-wave rectenna at 24 GHz for wearable IoT applications. They reported 2.5 V DC voltage at an input RF power of 18 dBm. Daskalakis *et al.* [10] developed a 24 GHz rectenna on paper substrate with a conversion efficiency of 32.5% at 15 dBm input power for RFID applications. Shinohara and Hatano [11] designed a rectifier circuit with a reported RF-DC conversion efficiency of 47.9% at an input power of 23 dBm. Laden *et al.* [6] presented the design and implementation of rectennas using substrate integrated waveguide (SIW) technology at 24 GHz. Their results showed that the rectification efficiency was 24% at an input power density of 10 mW/cm^2. Colado and Georgiadis [12] proposed an SIW-based rectenna at 24 GHz having a maximum RF-DC conversion efficiency of 15% at 8 dBm of input power. In [13] a 24 GHz rectenna was proposed for fixed wireless access applications with an RF-DC conversion efficiency of 43.6% at 27 dBm input power. In another research work for a similar application, an energy harvester at millimetre-wave frequencies was proposed [14]. It exhibited a measured RF-DC conversion efficiency of 67% and a maximum voltage of 2.18 V at 35.7 GHz.

In most of the above-mentioned research works the authors only presented the simulated RF-DC conversion efficiencies, which are generally higher than the actual measured results. The experimental RF-DC conversion efficiency of rectifiers and rectennas tends to be lower than the simulated one due to multiple factors such as lower gain and radiation efficiency of the antennas, lower than predicted input RF power to rectifiers, diode parasitic components, and the DC load resistance deviating from the optimum [1].

In parallel to these advancements, IoT technology is another still developing field which is expected to have a lot of practical applications in many industries, including agriculture, construction, manufacturing, healthcare, energy, and transportation. However, the batteries present in these devices have many drawbacks in terms of size, weight, and cost, in addition to requiring replacement once depleted. This, in turn, can make the installation of battery-powered devices in remote and hard-to-reach places, such as bridge bearings or along river beds, impractical. Hence, the battery life of an IoT device is one of the challenges that needs to be addressed before large-scale deployment is possible.

The solution proposed in this paper is to use a physically small energy storage element, e.g. a supercapacitor, which can be charged through wireless power transfer at 24 GHz. The motivation behind this research is to replace the need for a battery in sensor nodes deployed in places with limited accessibility. The sensor nodes themselves will then be able to wirelessly communicate with a base station using an energy-efficient method such as backscatter modulation. The block diagram of such a system is illustrated in Fig. 1.

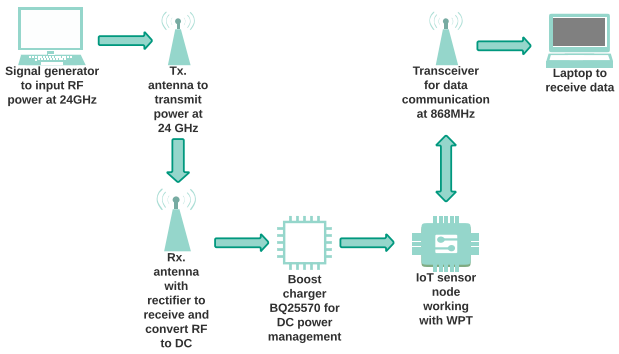

FIGURE 1. System block diagram of wireless power transfer to a battery-less sensor node.

In this paper, such a complete wireless information and power transfer system, operating at 24 GHz, is experimentally demonstrated for the purposes of charging a battery-less sensor node. The sensor uses the lower frequency of 868 MHz to wireless communicate data, as this is well suited for low-power, long-range communications.

The design, simulation and implementation of shunt and voltage-doubler rectifier circuits are presented, as well as a suitable antenna array. Initially, the array and the rectifier circuits are individually designed, optimised, fabricated, and measured. To form a complete rectenna layout, the antenna array and rectifier are integrated into one board, reducing the overall size of the WPT receiver. A comprehensive performance comparison of the different rectifier circuits follows, with a final demonstration of a battery-less sensor node fully powered by the rectenna completing this research work.

To the best of the authors' knowledge, this is the first time a complete wireless power transfer system for battery-less sensor nodes, operating in the ISM band 24 GHz, has been reported.

II. RECTIFIER DESIGNS & SIMULATION RESULTS

Microwave and millimetre-wave rectifiers can be implemented in various configurations, with the single-diode series and shunt ones being the most common. To increase the DC output voltage, one can also use a voltage-doubler, which requires two diodes.

The general topology of a rectifier consists of a source impedance matching network to match the power source to the input impedance of the circuit, a non-linear element which

converts the RF energy to DC energy, e.g. a Schottky diode, and a low-pass filter with a load resistance.

In this research work these two different rectifier configurations, i.e. shunt and voltage-doubler, have been evaluated with an input RF signal at 24 GHz, by using two different commercially available low-barrier height Schottky diodes, i.e. Macom MA4E2054A and Skyworks SMS7621. These diodes were chosen due to their extensive documentation, i.e. SPICE parameters for the intrinsic diode junctions and equivalent circuit models for their packages, and their availability in small packages with reduced parasitics.

The shunt configuration was chosen for two reasons. First, it is requires very few components and therefore occupies little board space. Second, it contains a natural closed DC loop independent of the input power source, whereas the series configuration requires additional elements to achieve that. The voltage-doubler was has similar properties to the shunt configuration, however it also exhibits higher DC output voltage, which is beneficial when the rectifier is connected to a power management circuit.

The Schottky diodes selected have both got low barrier height meaning they will exhibit non-linear behaviour at lower input power, have been successfully demonstrated in rectifier circuits at lower frequencies, and most importantly, are available in small packages. The last property makes them particularly suitable, due to decreased parasitics and physical size.

The main figure of merit for the performance of rectifiers is the RF-DC conversion efficiency defined as:

$$\eta = \frac{P_{out}}{P_{in}} \tag{1}$$

where P_{out} is the DC output power and P_{in} is the input RF power. Circuit parameters such as DC load resistance, smoothing and decoupling capacitors, source impedance matching networks and higher-order harmonic suppression radial stubs were optimised, using Keysight Advanced Design System (ADS), to obtain the maximum RF-DC conversion efficiency. The design of the rectifier circuits followed a well-established procedure, where the value of the DC load was swept, and a source-pull was performed for every value of DC resistance. This way optimal conditions were identified, and impedance matching networks were designed.

Following experimental measurements of the designed rectifiers, the circuit with highest RF-DC conversion efficiency was chosen to demonstrate the full wireless information and power transfer system.

A. RECTIFYING DIODES

In order to successfully design the rectifiers, the diodes need to be represented in the Keysight ADS Harmonic Balance simulator using their SPICE parameters. Furthermore, due to the high frequency of operation, i.e. 24 GHz, it is also important to include the circuit model of their respective packages.

These parameters are readily available from their respective datasheets [15], [16]. The final simulation models of these diodes and their packages are shown in Fig. 2a and Fig. 2b, and the most relevant SPICE parameters are included for reference in Table 1.

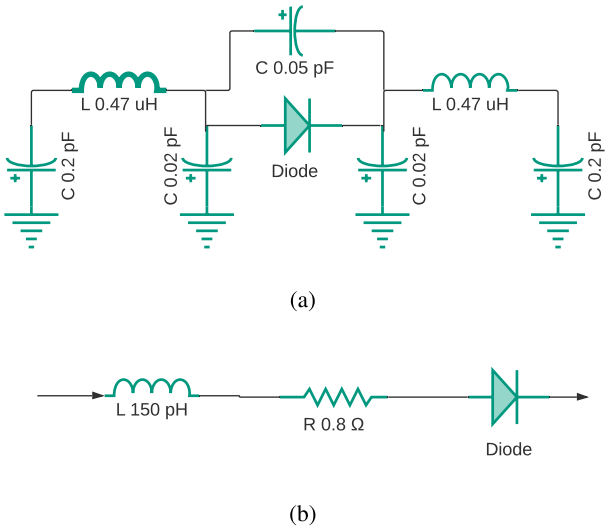

FIGURE 2. Diode package model a) SOD-323, b) 0201.

TABLE 1. Schottky diode SPICE parameters.

Parameter	MA4E2054A	SMS7621
Package	SOD-323	0201
R_s, Ω	10.5	10.3
C_{j0}, pF	0.13	0.13
V_{BR}, V	3.0	3.0
V_F, mV	250	260
I_F, mA	1	1

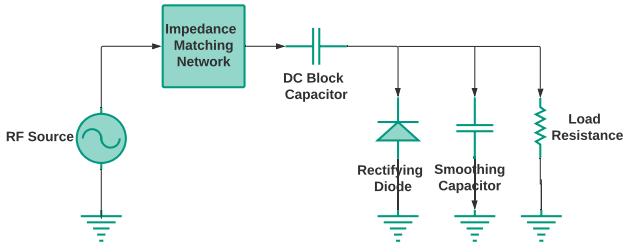

FIGURE 3. Rectifier circuit in shunt configuration.

B. SHUNT CONFIGURATION

The design of a rectifier in shunt configuration is shown in Fig. 3. In this configuration, the diode is mounted in parallel to the DC load resistance. The same circuit topology was used with the two different Schottky diodes to compare their performance in shunt configuration. Fig. 4 presents their

TABLE 2. Performance comparison of proposed rectifiers.

	Shunt	Voltage-doubler	Diode
RF-DC Conversion Efficiency (%)	46	36	MA4E2054A
	25	20	SMS7621
DC Output Voltage (V)	1.5	1.9	MA4E2054A
	1.1	1.4	SMS7621
Output Power (mW)	11.0	7.0	MA4E2054A
	5.5	3.5	SMS7621
Optimal Load Resistance (Ω)	200	400	MA4E2054A
	200	400	SMS7621

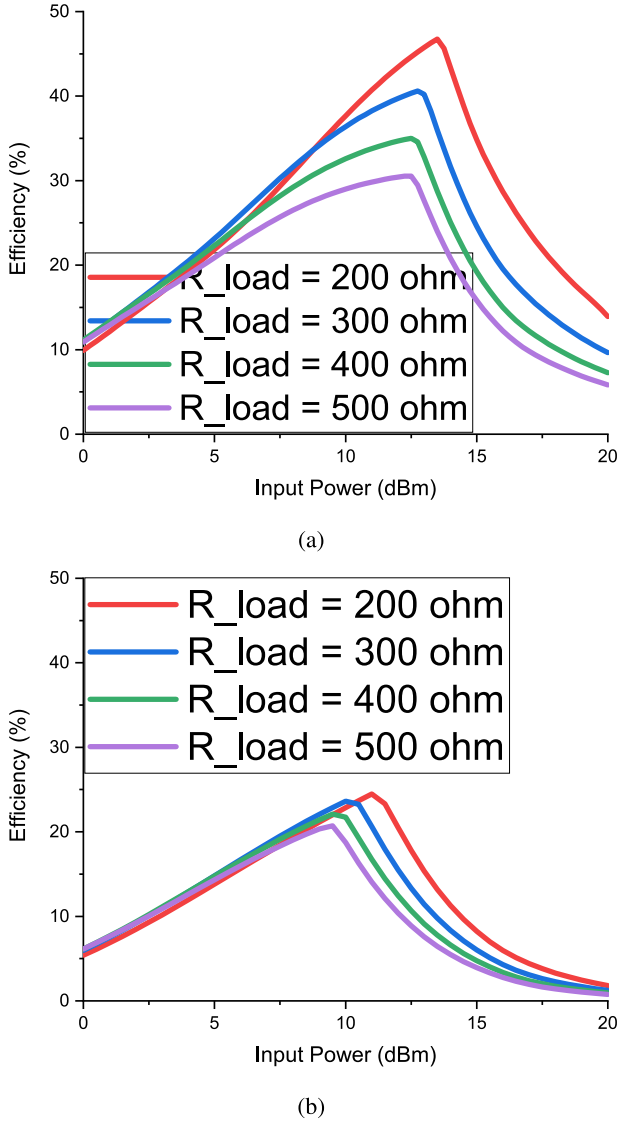

FIGURE 4. Simulated RF-DC conversion efficiency of shunt rectifiers as a function of input power and DC load resistance: a) MA4E2054A b) SMS7621.

simulated RF to DC conversion efficiency as a function of the DC load resistance R_{DC} and RF input power P_{IN}. It can be seen that the rectifier utilising the MA4E2054A diode achieves a maximum efficiency of 46% as compared to 25% for the one with the SMS7621 diode. In both cases, a 200 Ω DC load resistance was found to be the optimal one.

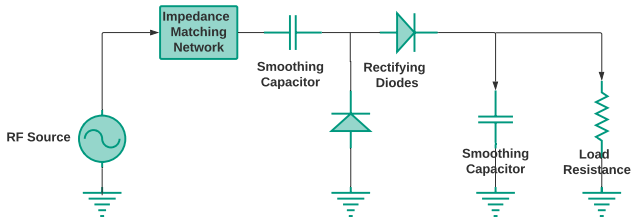

FIGURE 5. Rectifier circuit in voltage-doubler configuration.

C. VOLTAGE-DOUBLER CONFIGURATION

In the circuit topology illustrated in Fig. 5, two diodes are used to increase the output voltage and provide full-wave rectification [9]. The voltage doubler rectifier exhibits lower conversion efficiency for the same level of input RF power, when compared to the shunt configuration, due to twice the diode loss. Simulation results, presented in Fig. 6, show that the voltage-doubler provides a maximum rectification efficiency of 36% or 22% with the MA4E2054A or SMS7621 diode, respectively, for a 400 Ω DC load resistance and 12.5 dBm input power.

D. COMPARISON OF RECTIFIER CONFIGURATIONS

In this section we present a performance comparison in terms of simulated RF-DC conversion efficiency of the two rectifier configurations using the two different diodes. It is evident that the rectifier in shunt configuration using a MA4E2054A Schottky diode performs best, yielding a maximum efficiency of 46% for a load resistance of 200 Ω and RF input power of 14 dBm.

However, the voltage-doubler circuits have a higher DC output voltage compared to the shunt ones, for both diodes. A trade-off decision might be necessary depending on the minimum input voltage requirements of the next stage in a system, which is normally a power management circuit.

A full performance comparison and design parameters along with the values of the proposed rectifiers are summarised in Table 2.

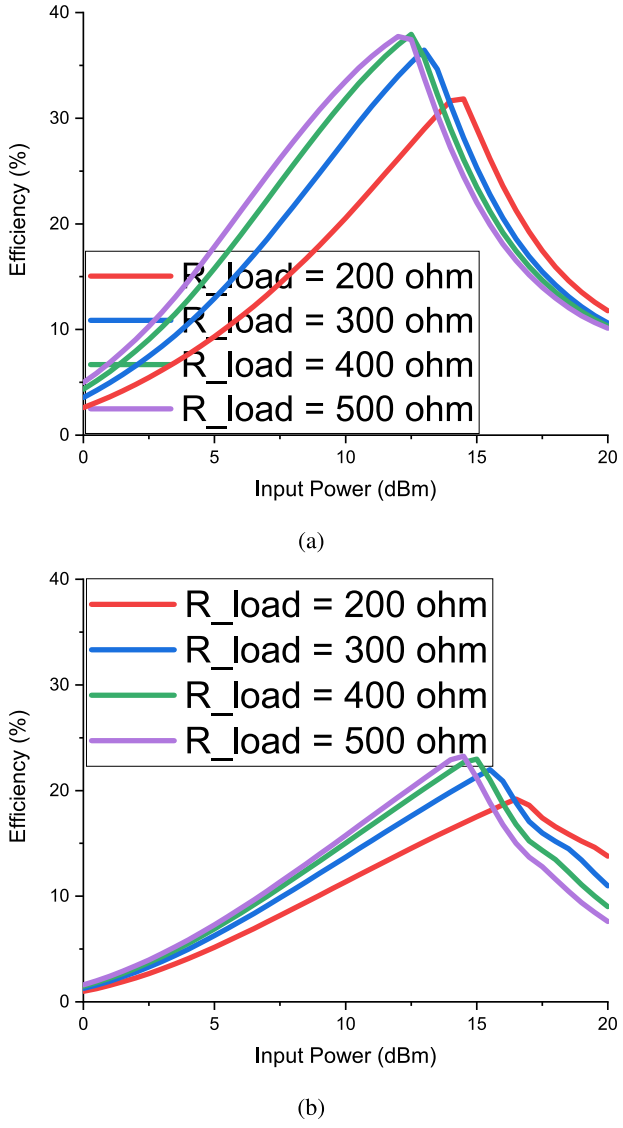

FIGURE 6. Simulated RF-DC conversion efficiency of voltage-doubler rectifiers as a function of input power and DC load resistance: a) MA4E2054A b) SMS7621.

III. ANTENNA ARRAY DESIGN FOR WPT

A 4 × 4 microstrip patch antenna (MPA) array was designed, to receive the RF power and transfer it to the rectifier circuit. This configuration was chosen as a compromise between expected gain, aperture size, and minimum operating distance as required by the far-field region relationship:

$$R \geq \frac{2D^2}{\lambda} \tag{2}$$

where D is the largest linear dimension of the antenna array and λ is the free-space wavelength of the frequency of operation.

The proposed MPA array layout with main dimensions and a fabricated sample are shown in Fig. 7. A combination of corporate and series feed network was designed to connect the patches. Rogers 3003 substrate material with thickness 0.51 mm, $\epsilon_r = 3.0$ and loss tangent $\tan\delta = 0.001$ was used.

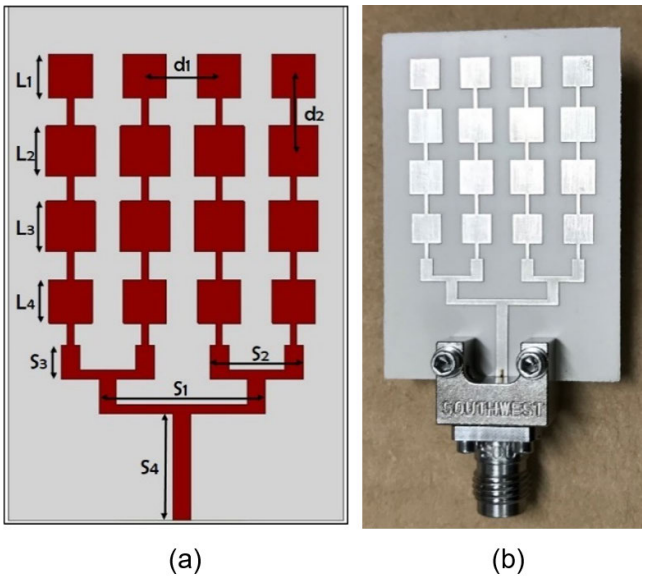

FIGURE 7. Planar 4 × 4 MPA array, a). Array layout with dimensions L1=L4=3.5 mm, L2=L3=4 mm, d1=d2=6 mm, S1=13.4 mm, S2=7.5 mm, S3=2.7 mm, S4=8.55 mm, b). Fabricated array.

The input match of the fabricated arrays was measured in laboratory conditions using a Keysight N5247A PNA-X with 1-port Short, Open, Load (SOL) calibration, bringing the S-parameter reference plane to the end of the coaxial cable. Data was taken over the frequency range of interest, i.e. 22 GHz - 26 GHz, with 1001 frequency points. The radiation pattern and realised gain were measured in an anechoic chamber using the gain transfer method and two standard gain pyramidal horn antennas.

A comparison between the measured and simulated S-parameters and radiation pattern of the proposed MPA array are presented in Fig. 8 and Fig. 9, respectively. The results show a maximum realised gain of 13.8 dBi and a fractional bandwidth of more than 9% at 24 GHz.

IV. EXPERIMENTAL RESULTS

A. STANDALONE RECTIFIERS

After analysing the simulation results of the different rectifiers, the shunt and voltage-doubler configurations with a MA4E2054A Schottky diode were selected for fabrication, with samples shown in Fig. 10. The circuits were fabricated on a 0.51 mm thick Rogers 3003 substrate, the same one that was used for the antenna arrays.

Precision field-replaceable 2.4 mm Southwest Microwave connectors were used to connect the circuits to the coaxial-based measurement equipment. The circuits were measured using a Keysight E8267D Signal Generator set at 24 GHz. The output voltage of the rectifier was measured using a digital multimetre at the optimal load resistances of 200 Ω and 400 Ω for shunt and voltage-doubler configurations, respectively. The comparison of measured and simulated RF-DC conversion efficiency with respect to the level of RF input power is depicted in Fig. 11 and Fig. 12.

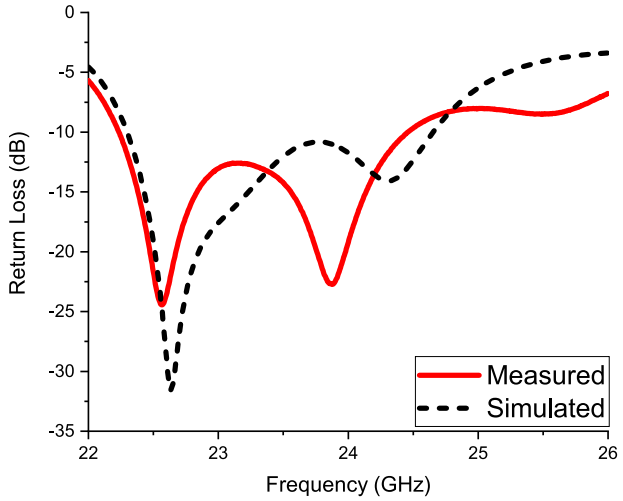

FIGURE 8. Simulated and measured return loss performance.

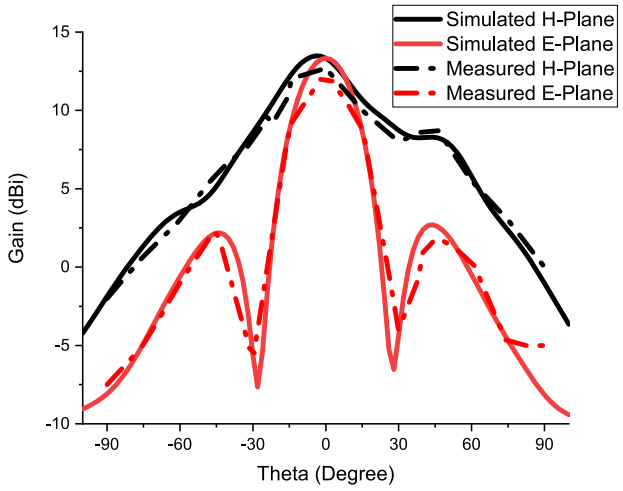

FIGURE 9. Simulated and measured E-plane and H-plane radiation pattern.

The differences between the simulated and measured results are attributed to the following reasons: (i) The simulation results were obtained from Keysight ADS and the end-launch connector was not included in the simulation model; (ii) Fabrication tolerances, imperfect manual placement of parts, and soldering effects have shifted the optimum input impedance and DC load requirements.

In any case, the experimentally obtained maximum rectification efficiencies, 35% at 18 dBm input power for the shunt rectifier, and 30% at 16 dBm input power for the voltage-doubler version, are between six and ten percentage points better than the state-of-the-art, as summarised in Table 3.

B. COMBINED RECTIFIERS AND ANTENNAS (Rectennas)

In this section the measurements of rectifier circuits integrated with antenna arrays to form a complete rectenna for WPT at 24 GHz are presented and discussed. An example of a fabricated rectenna, along with an illustration of the measurement setup are shown in Fig. 13 and Fig. 14, respectively.

A transmitter antenna, in this case a WR-28 standard gain pyramidal horn, was connected to the signal generator, the output power of which was varied between 0 dBm and 20 dBm in 2 dBm steps at the frequency of interest, i.e. 24 GHz. The maximum output power was limited to 20 dBm due to the capabilities of the signal generator. On the receiver side, the proposed rectenna was mounted at a dis-

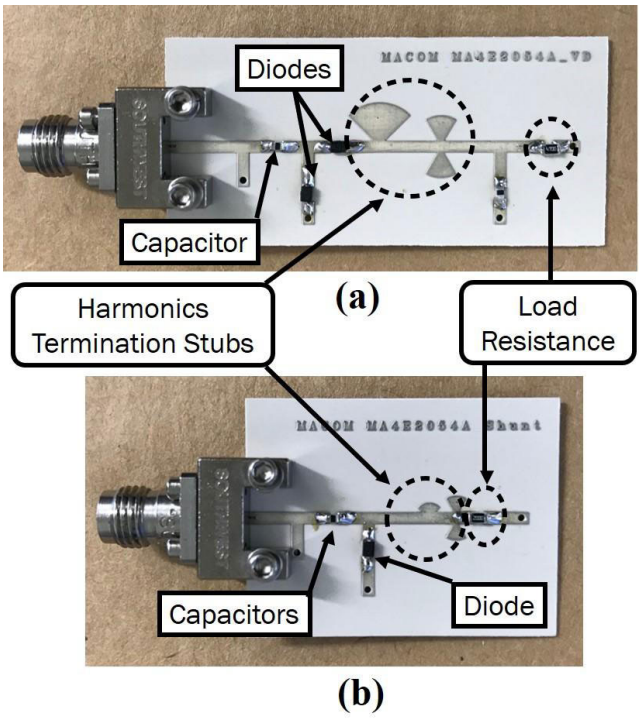

FIGURE 10. Fabricated rectifier circuits a) voltage-doubler, b) shunt.

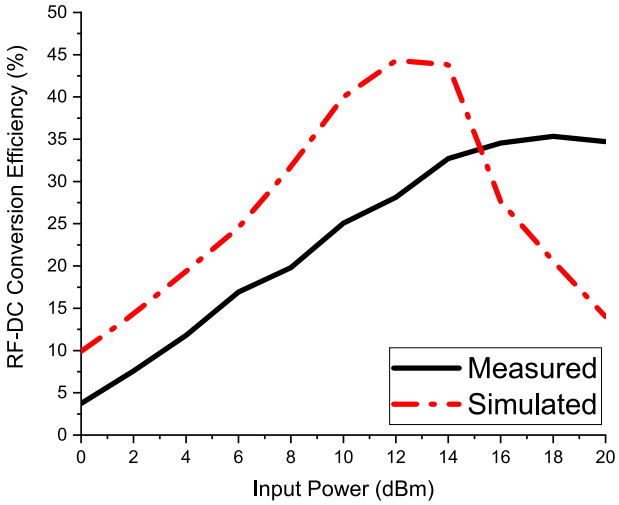

FIGURE 11. Measured RF-DC conversion efficiency of rectifier in shunt configuration as a function of input power.

TABLE 3. Summary of published rectenna performance at or above 24 GHz.

Ref	Efficiency (%)	DC Output (V)	Frequency (GHz)	Input Power (dBm)
[6]	24	0.6	24	18
[10]	-	0.29	24	18
[11]	35 (sim)	-	24	15
[12]	43.6 (sim)	-	24	27
[13]	16.2	-	24	8
[18]	40 (sim)	-	24	35
[15]	67 (sim)	2.2	35	7
This Work	35	2.5	24	18

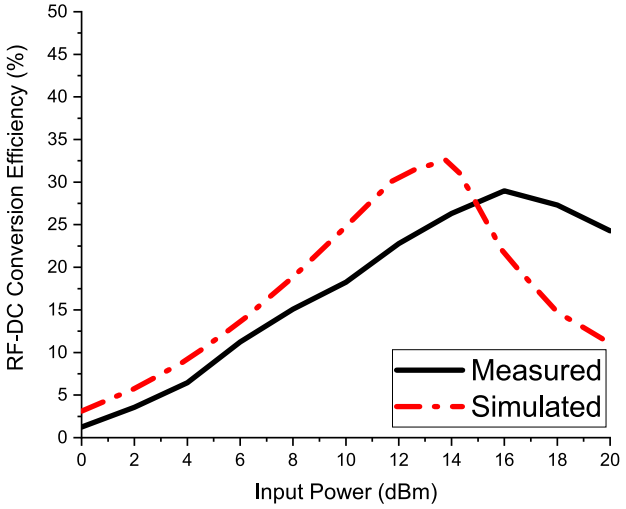

FIGURE 12. Measured RF-DC conversion efficiency of rectifier in voltage-doubler configuration as a function of input power.

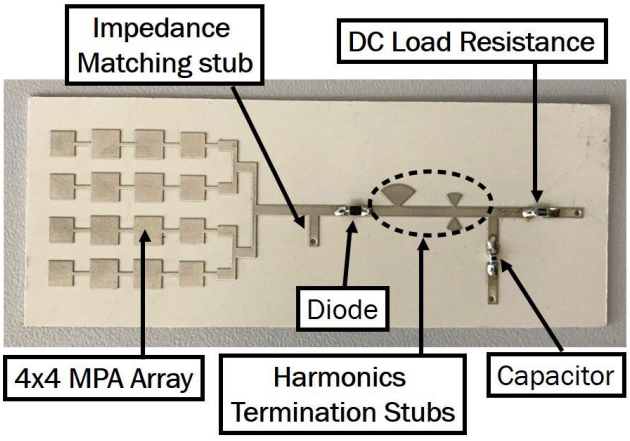

FIGURE 13. Fabricated rectenna sample.

tance of 0.15 m, which was chosen as it is greater than the minimum far-field distance (0.14 m) of both the pyramidal horn and the microstrip patch array. Fig. 15 shows the experimental results of the rectenna, i.e. the obtained DC power and efficiency as a function of the RF power at the output of the

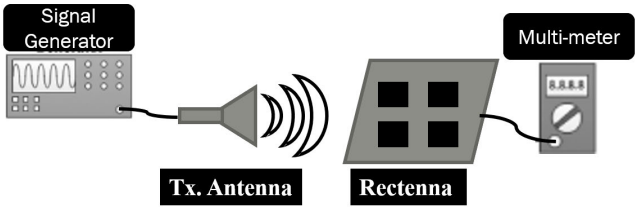

FIGURE 14. Illustration of the measurement setup for rectennas.

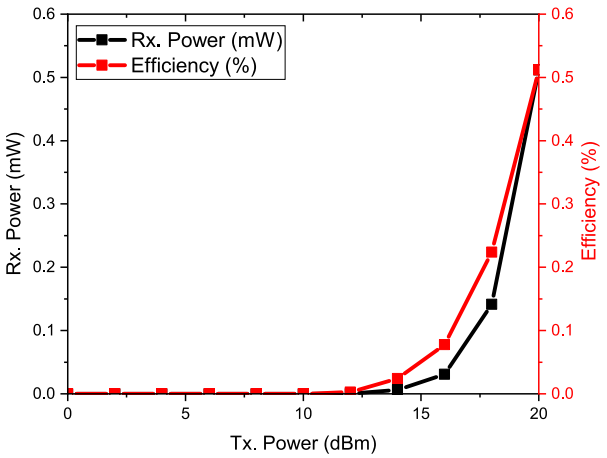

FIGURE 15. Measured output power and RF-DC conversion efficiency of proposed rectenna at 24 GHz as a function of input power at a distance of 0.15 m.

signal generator. A maximum DC output power of 0.51 mW was achieved for a RF transmit power of 20 dBm (100 mW) at the specified distance of 0.15 m.

The maximum experimental overall efficiency of this WPT system is 0.5%. Compared to the individual efficiencies of the transmit and receive antennas and the rectifiers, this is quite low. However, it is dominated by propagation and atmospheric losses, meaning that the RF power reaching the rectifier would be much lower than its optimal conditions.

To illustrate the above point, a simplified link budget calculation is presented next. In addition to the P_{TX} of 20 dBm and the G_{RX} of 13.8 dBi, the gain of the horn antenna (G_{TX}) is 17.1 dBi per its datasheet, and all cable and connector

losses are assumed to add to 1 dB. The free-space path loss at 24 GHz for a distance of 0.15 m is calculated to be 43.6 dB. Putting all these together yields:

$$\begin{aligned} P_{RX} &= P_{TX} - L_{MISC} + G_{TX} - L_{FSPL} + G_{RX} \\ &= 20 - 1 + 17.1 - 43.6 + 13.8 \\ &= 6.3\,dBm \end{aligned} \tag{3}$$

Looking at the measured performance of the shunt rectifier (Fig. 11), for the rectification efficiency for that input RF power level is expected to be around 15%, meaning a DC power of $4.27 \times 0.15 = 0.64$ mW will be expected at the output of the rectenna. Instead, the measured DC power is 0.51 mW, which corresponds to a received RF power level of between 5.5 dBm and 5.8 dBm, again looking at the measured rectification performance. This difference of 0.5 dB – 0.8 dB can collectively be attributed to additional losses, including in the DC measurement equipment and uncertainties in measurement results. In any case, the system measurement results correlate well with this quick modelling.

One approach to address this would be to increase the power at the transmitter, provided the equipment to do so is available. An alternative approach, and the one adopted in the next section, would be to transmit power for a longer duration, which would still achieve the goal of providing sufficient energy to the battery-less sensor node.

V. DEMONSTRATION OF A COMPLETE WPT SYSTEM FOR IoT SENSOR NODES

In this section the proposed rectennas are used for the practical demonstration of wireless power transfer to a battery-less sensor node which can communicate sensor data via backscatter modulation. The measurement setup is shown in Fig. 16. It consists of an RF source transmitting power to the node at 24 GHz in order to provide enough energy for it to activate and take a single measurement. This way, the need for batteries can be eliminated.

The rest of the system modules used in this demonstration are: (i) the proposed rectifier in shunt configuration with a 4×4 planar microstrip patch antenna array, as illustrated in Fig. 13; (ii) power management module (Texas Instruments BQ25570), which uses a 4.7 mF capacitor to store the DC energy; (iii) a sensor node that uses a low-power microcontroller to implement backscatter communication at 868 MHz; and (iv) a Nuand BladeRF Software Defined Radio (SDR) module which acts as a receiver for the sensor node data. It was experimentally determined that the sensor node board requires 5 J of energy to wake up and transmit a data packet to the SDR base station, a task that takes approximately 2 seconds. Given the characteristics of the rectenna subsystem, 10 seconds were needed before that amount of energy was transferred to the 4.7 mF capacitor.

In our sensor node design, the backscatter modulation is driven by the payload data packets generated by an ultra-low power microcontroller unit (MCU), such as Texas Instruments MSP430 or an ST Microelectronics ARM M0+. These

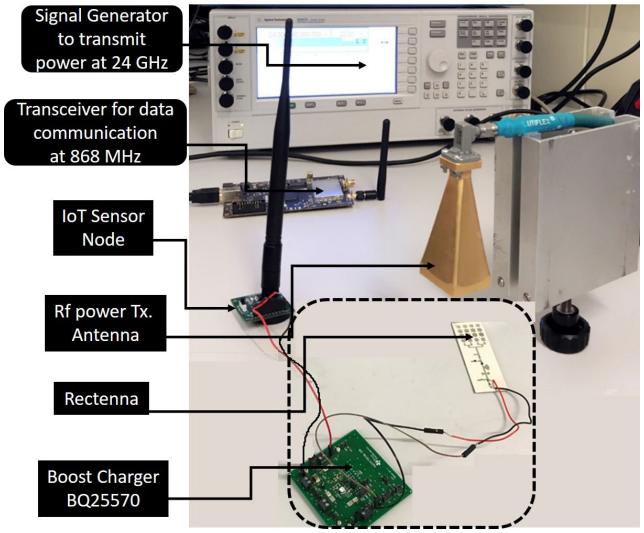

FIGURE 16. Measurement setup for WPT to a battery-less sensor node, containing all the system components. The sensor node is outlined as the figure has been edited for compactness.

MCUs are suitable as their active mode current requirements can be as low as several μA. For the purposes of the system demonstration and evaluation, the MCU generated a stream of random bits which were subsequently transmitted using backscatter modulation.

However, in a future system, sensors could be incorporated, connecting with the MCU using interfaces such as I2C or SPI. For example, a widely-used temperature sensor such as Texas Instruments TMP117, operates at 3.3 V, requires 135 μA supply current, and takes 16 ms to complete one measurement [18]. Supplying enough energy for such a sensor would require an additional 60-70 ms long transmission, using the current combination of WPT transmitter and receiver.

The bladeRF module is used to generate a continuous wave (CW) signal at 868 MHz, with an output power of 14 dBm, which is modulated by the sensor node. The energy harvested by the rectenna is then used to power the MCU of the sensor node, which is responsible for modulating the 868 MHz by switching between two different RF loads, thereby changing the amount of reflected RF energy.

In a nutshell, our load modulation scheme translates to amplitude shift keying (ASK), with binary 0 associated with high reflection and binary 1 with low reflection. The modulated signal is also received and decoded by the SDR module. The achieved data rate using this setup was 2400 bps.

Fig. 17 shows an example of data received from the battery-less sensor node that was energised by wireless power transfer at 24 GHz. The unipolar signal is the received modulated data and the bipolar one represents the decoded data after level detection.

This approach combines the advantages of 24 GHz for WPT with the low-cost, low-power wireless communications off-the-shelf hardware at 868 MHz for data transfer.

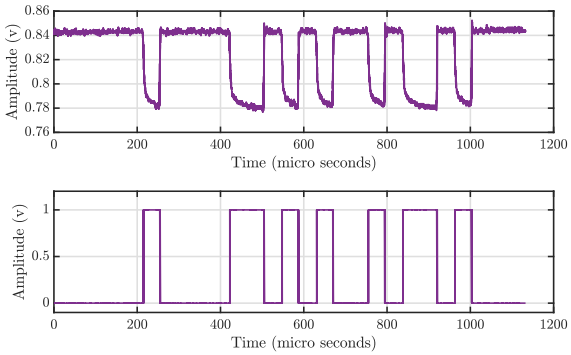

FIGURE 17. Data received from the wirelessly powered sensor node, showing both raw signal and decoded digital data.

It is important at this stage to discuss the potential limits and parameters within which this system can operate. For example, the maximum distance between the RF power transmitter and WPT receiver that could be achieved depends on many factors. The first and main one is the maximum RF Tx EIRP, which is normally fixed by individual countries' regulators. In the case of the UK, at 24 GHz the maximum EIRP is 100 mW, or 20 dBm, as per Ofcom Interface Requirement 2030 [19].

Whilst this limit cannot be currently exceeded, the size, and thereby gain, of the receive antenna can be controlled. Another approach to increasing the range will be the use of dielectric lens to increase the directivity of the receive antennas. Unfortunately, doing that will also increase the minimum link distance. This discussion forms part of a work in progress by the authors.

A further aspect is the duration for which power can be transmitted. A sensor node could require two seconds of power transmission to wake up and take a single measurement, or it might require 10 seconds. For example, in the case of a UAV-based platform, the former case will be preferable, whereas if the system is integrated with a land robot the latter might still be acceptable. The end applications that the authors have presented that would be enabled are still the same, i.e. battery-less sensor nodes. More precise modelling and calculations will be included in the previously mentioned work in progress.

VI. CONCLUSION

A complete wireless power transfer system for battery-less sensor nodes at 24 GHz has been presented. The RF-DC conversion efficiency of two different rectifier topologies using two different Schottky diodes was examined. Based on the simulation results, the rectifier circuit with maximum RF-DC conversion efficiency was chosen as the rectifying component in the WPT system. A 4×4 MPA array and the rectifier circuits were fabricated and measured separately to verify the performance of the individual components.

For the standalone rectifier, a maximum output DC voltage of 2.5 V with an RF-DC conversion efficiency of 35% was observed at 200 Ω load resistance with 16 dBm input power at 24 GHz, which is a significant improvement on the state-of-the-art. The 4×4 MPA array had a measured gain of 13.8 dBi and good return loss at the frequency of interest.

The designed antenna and rectifier were integrated together and fabricated on a single board to validate the rectenna performance. The obtained results present a significant enhancement in the design of high-efficiency WPT rectennas. Finally, the application of the system to low-power battery-less sensor nodes was demonstrated by wirelessly charging a custom sensor that communicates useful information via backscatter modulation.

In principle, the proposed system is well-suited for millimetre-wave far-field wireless power transfer for sensor nodes, robotics, and healthcare applications. The proposed rectennas have high RF-DC conversion efficiency as well as a highly directional radiation pattern with a corresponding high gain and low side lobe levels, helping reduce interference.

Example applications include using a UAV to transmit RF power to sensor nodes and then receive the sensor data in a few seconds. Additional applications for the range-limited version demonstrated in this paper could be using land robots or robotic arms for short-distance, contactless interrogation of sensor nodes.

To summarise, both simulation and measurement results of a complete wireless power transfer system for battery-less sensor nodes have been presented and discussed here. To the best of the authors' knowledge, this is the first such system operating in the 24 GHz ISM frequency band.

REFERENCES

[1] S. Mizojiri and K. Shimamura, "Wireless power transfer via subterahertz-wave," *Appl. Sci.*, vol. 8, no. 12, p. 2653, Dec. 2018.
[2] Q. Zhang, J.-H. Ou, Z. Wu, and H.-Z. Tan, "Novel microwave rectifier optimizing method and its application in rectenna designs," *IEEE Access*, vol. 6, pp. 53557–53565, 2018.
[3] Mutee-Ur-Rehman, W. Ahmad, M. I. Qureshi, and W. T. Khan, "A highly efficient tri band (GSM1800, WiFi2400 and WiFi5000) rectifier for various radio frequency harvesting applications," in *Proc. Prog. Electromagn. Res. Symp. Fall (PIERS-FALL)*, Nov. 2017, pp. 2039–2044. [Online]. Available: https://ieeexplore.ieee.org/document/8293473/authors#authors
[4] T. Matsunaga, E. Nishiyama, and I. Toyoda, "5.8-GHz stacked differential rectenna suitable for large-scale rectenna arrays with DC connection," *IEEE Trans. Antennas Propag.*, vol. 63, no. 12, pp. 5944–5949, Dec. 2015.
[5] N. Shinohara, "Rectennas for microwave power transmission," *IEICE Electron. Exp.*, vol. 10, no. 21, p. 20132009, 2013.
[6] S. Ladan, A. B. Guntupalli, and K. Wu, "A high-efficiency 24 GHz rectenna development towards millimeter-wave energy harvesting and wireless power transmission," *IEEE Trans. Circuits Syst. I, Reg. Papers*, vol. 61, no. 12, pp. 3358–3366, Dec. 2014.
[7] International Commission on Non-Ionizing Radiation Protection, "ICNIRP statement on the 'guidelines for limiting exposure to time-varying electric, magnetic, and electromagnetic fields (up to 300 ghz),'" *Health Phys.*, vol. 97, no. 3, pp. 257–258, 2009.
[8] M. Moradi, N. Naghdi, H. Hemmati, M. Asadi-Samani, and M. Bahmani, "Effect of ultra high frequency mobile phone radiation on human health," *Electron. Phys.*, vol. 8, no. 5, p. 2452, 2016.
[9] J. Bito, V. Palazzi, J. Hester, R. Bahr, F. Alimenti, P. Mezzanotte, L. Roselli, and M. M. Tentzeris, "Millimeter-wave ink-jet printed RF energy harvester for next generation flexible electronics," in *Proc. IEEE Wireless Power Transf. Conf. (WPTC)*, May 2017, pp. 1–4.
[10] S. Daskalakis, J. Kimionis, J. Hester, A. Collado, M. M. Tentzeris, and A. Georgiadis, "Inkjet printed 24 GHz rectenna on paper for millimeter wave identification and wireless power transfer applications," in *IEEE MTT-S Int. Microw. Symp. Dig.*, Sep. 2017, pp. 1–3.

[11] N. Shinohara and K. Hatano, "Development of 24GHz rectenna for receiving and rectifying modulated waves," *J. Phys., Conf. Ser.*, vol. 557, Nov. 2014, Art. no. 012002.
[12] A. Collado and A. Georgiadis, "24 GHz substrate integrated waveguide (SIW) rectenna for energy harvesting and wireless power transmission," in *IEEE MTT-S Int. Microw. Symp. Dig.*, Jun. 2013, pp. 1–3.
[13] N. Shinohara, K. Nishikawa, T. Seki, and K. Hiraga, "Development of 24 GHz rectennas for fixed wireless access," in *Proc. 30th URSI Gen. Assem. Sci. Symp.*, Aug. 2011, pp. 1–4.
[14] A. Mavaddat, S. H. M. Armaki, and A. R. Erfanian, "Millimeter-wave energy harvesting using 4×4 microstrip patch antenna array," *IEEE Antennas Wireless Propag. Lett.*, vol. 14, pp. 515–518, 2014.
[15] *Mouser Data Sheet*. Accessed: Nov. 4,2019. [Online]. Available: https://www.mouser.com/datasheet/2/249/MA4E2054_Series-475823.pdf
[16] *Skyworks: Surface Mount, 0201 Low-Barrier Silicon Schottky Diode*. Accessed: Nov. 4, 2019. [Online]. Available: https://www.skyworksinc.com/products/diodes/sms7621-060
[17] S. Ladan, S. Hemour, and K. Wu, "Towards millimeter-wave high-efficiency rectification for wireless energy harvesting," in *Proc. IEEE Int. Wireless Symp. (IWS)*, Apr. 2013, pp. 1–4.
[18] *Tmp117 Data Sheet*. Accessed: May 16, 2020. [Online]. Available: http://www.ti.com/lit/ds/symlink/tmp117.pdf
[19] "IR 2030–UK interface requirements 2030," Ofcom, London, U.K., Tech. Rep., Nov. 2018.

BILAL TARIQ MALIK (Graduate Student Member, IEEE) received the B.Sc. and M.Sc. degrees from the Department of Electrical Engineering, COMSATS University Islamabad, Pakistan, in 2011 and 2014, respectively, and the Ph.D. degree in electronics and electrical engineering from the University of Leeds, U.K., in 2019.

He is currently with the COMSATS University Islamabad. He is currently a Research Fellow of the Advanced Technology Institute (ATI), University of Surrey, Guildford, U.K. His research interests include millimeter-wave antenna arrays, flexible printed circuits, rectennas for far-field wireless power transfer, and 5G communications. He was awarded the Institute Silver Medal and the Campus Bronze Medal for the B.Sc. degree from the COMSATS University Islamabad.

VIKTOR DOYCHINOV received the B.Eng. degree in telecommunications from the Technical University of Sofia, Bulgaria, in 2009, the M.Sc. degree in spacecraft technology and satellite communications from University College London, U.K., in 2011, and the Ph.D. degree in electronics and electrical engineering from the University of Leeds, U.K., in 2016.

Since 2016, he has been a Research Fellow of the School of Electronics and Electrical Engineering, University of Leeds, where he has been involved in the field of high-frequency engineering. His current research interests include microwave and millimeter-wave circuits and antennas, biomedical applications of wireless technology, and wireless communications in complex environments.

ALI MOHAMMAD HAYAJNEH (Member, IEEE) received the B.E. and M.Sc. degrees from the Department of Electrical Engineering, Jordan University of Science and Technology, Jordan, and the Ph.D. degree in electronics and electrical engineering from the University of Leeds, U.K.

He is working as an Assistant Professor with The Hashemite University, Jordan. His current research interests include drone-assisted wireless communication, public safety communication networks, stochastic geometry, device-to-device and machine-to-machine communication, and the modeling of heterogeneous networks, cognitive radio networks, and cooperative relaying networks.

SYED ALI RAZA ZAIDI (Member, IEEE) received the Ph.D. degree from the School of Electronics and Electrical Engineering, University of Leeds, Leeds.

From 2011 to 2013, he was associated with the International University of Rabat as a Lecturer. From 2013 to 2015, he was associated with the SPCOM Research Group, U.S. Army Research Laboratory, and a funded project in the area of network science. In 2013, he was also a Visiting Research Scientist with the Qatar Innovations and Mobility Centre, where he was involved in QNRF funded project QSON. He is currently a University Academic Fellow (Assistant Professor) of wireless communication and sensing systems with the University of Leeds. He has published over 90 articles in leading IEEE conferences and journals.

Dr. Zaidi is also an active member of the EPSRC Peer Review College. During the Ph.D. degree, he received the G. W. Carter Prize and the F. W. Carter Prize for the best thesis and best research paper, respectively. He is a EURASIP Local Liaison in the U.K. and also a General Secretary of the IEEE Technical Subcommittee on Backhaul and Fronthaul networks. From 2014 to 2015, he served as an Editor for the IEEE COMMUNICATION LETTERS. He was also a Lead Guest Editor of *IET Signal Processing* journal's special issue on signal processing for large-scale 5G wireless networks. He is currently an Associate Technical Editor of the *IEEE Communication Magazine*.

IAN D. ROBERTSON (Fellow, IEEE) received the B.Sc.Eng. and Ph.D. degrees from King's College London, London, U.K., in 1984 and 1990, respectively.

From 1984 to 1986, he was with the GaAs MMIC Research Group, Plessey Research, and Caswell, U.K. After that, he returned to King's College London, initially as a Research Assistant, worked on the T-SAT Project, subsequently as a Lecturer, led the MMIC Research Team, and became a Reader, in 1994. In 1998, he became a Professor of microwave subsystems engineering with the University of Surrey, where he established the Microwave Systems Research Group and was a Founding Member of the Advanced Technology Institute. In 2004, he was appointed as the Centenary Chair of microwave and millimeter-wave circuits with the University of Leeds. He was the director of learning and teaching, from 2006 to 2011, and also the head of the school, from 2011 to 2016.

Prof. Robertson was the General Technical Programme Committee Chair of the European Microwave Week, in 2011 and 2016.

NUTAPONG SOMJIT (Senior Member, IEEE) received the Dipl.-Ing. (M.Sc.) degree from the Dresden University of Technology, in 2005, and the Ph.D. degree from the KTH Royal Institute of Technology, in 2012.

He returned to Dresden to lead a research team in micro-sensors and MEMS ICs for the Chair for Circuit Design and Network Theory. In 2013, he was appointed as a Lecturer (Assistant Professor) with the School of Electronic and Electrical Engineering, University of Leeds, where he is currently an Associate Professor/Reader. His main research focuses on integrated smart high-frequency components, heterogeneous integration and low-cost microfabrication processes.

Dr. Somjit was appointed a member of the Engineering, Physical, and Space Science Research Panel of the British Council, in 2014. He was a recipient of the Best Paper Award (EuMIC prize) with the European Microwave Week, in 2009. He was awarded a Graduate Fellowship from the IEEE Microwave Theory and Techniques Society (MTT-S), in 2010 and 2011, and the IEEE Doctoral Research Award from the IEEE Antennas and Propagation Society, in 2012. In 2016, he was the Chair of the Student Design Competition for the European Microwave Week and, in 2018, he was appointed an Associate Editor of IET Electronics. Since 2013, he has been a member of the International Editorial Board of the *International Journal of Applied Science and Technology*.